

Dynamic functional connectivity analysis in individuals with Autism Spectrum Disorder

Pindi Krishna Chandra Prasad
krishna.chandra@research.iiit.ac.in
IIIT Hyderabad

Kamalaker Dadi
kamalaker.dadi@research.iiit.ac.in
iHub-Data,IIIT Hyderabad

Bapi Raju Surampudi
raju.bapi@iiit.ac.in
IIIT Hyderabad

Abstract—Autism spectrum disorder (ASD) is a neurodevelopmental disorder that predominantly occurs in children. Previous brain research in ASD has mainly studied biomarkers based on the functional connectivity characterized by the correlation of static temporal signals. However, brain connectivity is dynamic and varies extensively among brain states. The main aim of the paper is to understand the fundamental group differences between ASD patients and typically developing (TD) subjects using dynamic functional connectivity (dFNC) analysis. In this study, we investigated the dFNC between 53 independent components among 188 ASD and 195 TD subjects. We estimated dFNC using sliding window-based approaches and identified four distinct dynamic states through hard-clustering analysis. Hyper-connectivity within the cognitive control domain, between cognitive control and default mode network, has been identified among ASD subjects. Hyper-connectivity within the default mode network has been found among TD individuals. Further, we estimated the dynamic temporal properties such as fractional time spent, and mean dwell time per state and observed significant differences between ASD and TD groups. ASD subjects are found to have significantly longer dwell time in state 4 when compared to TD individuals. We also found a significantly increased occurrence of state 4 in ASD subjects and states 1 and 3 in TD subjects. While there is broad consensus in the brain network profiles between static functional connectivity (sFNC) and dFNC, the temporal profile of brain state dynamics is additionally available with dFNC analysis and may potentially contribute to disease biomarkers.

Index Terms—Dynamic functional connectivity, Autism Spectrum Disorders, Autism Biomarkers

I. INTRODUCTION & RELATED WORK

Autism Spectrum Disorder (ASD) is a lifelong heterogeneous developmental disorder that is characterized by abnormal development of the brain. Deficits in social skills, incapability to articulate language, abnormal sensory-motor movements and stereotyped behaviors is mainly observed in children with ASD. It has been demonstrated that the non-invasive method, resting-state functional magnetic resonance imaging (rs-fMRI), which represents intrinsic brain activity, is useful for examining the neural mechanisms underlying neurological diseases [1]. Most previous studies associated ASD with atypical functional connectivity (FC) between different pairs of regions using traditional static methods based on rs-fMRI. Most of these studies assume brain connectivity is static. However, previous studies have hypothesized that the brain is inherently dynamic, frequently switching between discrete FC patterns during acquisition [2].

In contrast to static functional connectivity (sFNC) analysis, the dynamic properties of FC offer a novel perspective on the temporal features of activations across brain networks [3]. Presently dynamic functional network connectivity (dFNC) analysis has shown to be a successful procedure for examining the neurological underpinnings of several psychiatric disorders, including ASD. The blood-oxygen-level-dependent (BOLD) signals in the rs-fMRI time series were used to generate a functional correlation matrix for each overlapping interval. Over time, the alterations of FC between brain regions may be seen continuously [4], [5].

Fu et al. [6] investigated the dFNC between 51 intrinsic connectivity networks in 170 ASD subjects and 195 age-matched typically developing (TD) individuals. Hard clustering analysis on the dFNC windows has yielded five dynamic brain states that identified hyper-connectivity between subcortical (hypothalamus/subthalamus) and sensory-motor networks (lingual gyrus, paracentral lobule, and right postcentral gyrus), predominantly in certain states. Similarly, Ma et al. [7] identified several brain regions with dFNC analysis that showed higher inter-network functional connectivity between the central executive network (CEN), the ventral visual network (VVN) and attention network (AN) in ASD patients while comparing dFNC patterns among 88 ASD and 87 TD subjects. Interestingly, the same study by Ma et al. [7] did not observe any significant group differences with sFNC analysis which indicates the benefit of dFNC in revealing more sensitive brain regions in ASD subjects due to its temporal characteristics when compared to sFNC. Harlalka et al. [8] explored the dynamic alterations in the connection strength and dynamic properties like temporal modularity to characterize the differences between 100 ASD and 75 TD subjects. [8] found high correlation of symptom severity scores with these dFNC network-level temporal properties in ASD compared to TD subjects. Another study by Li et al. [9] compared variability in the temporal metrics on dFNC and clustering analysis to reveal the high variability of temporal metrics between the middle temporal pole and the posterior cingulate gyrus in ASD and its correlation to symptom severity.

Using the sliding window, hard clustering-based approaches, many studies investigated altered dFNC patterns in other disorders such as Parkinson's disease (PD), Subjective Cognitive Decline (SCD) and healthy controls (HCs). Chen et al. [10] investigated the dFNC and static parameters obtained from

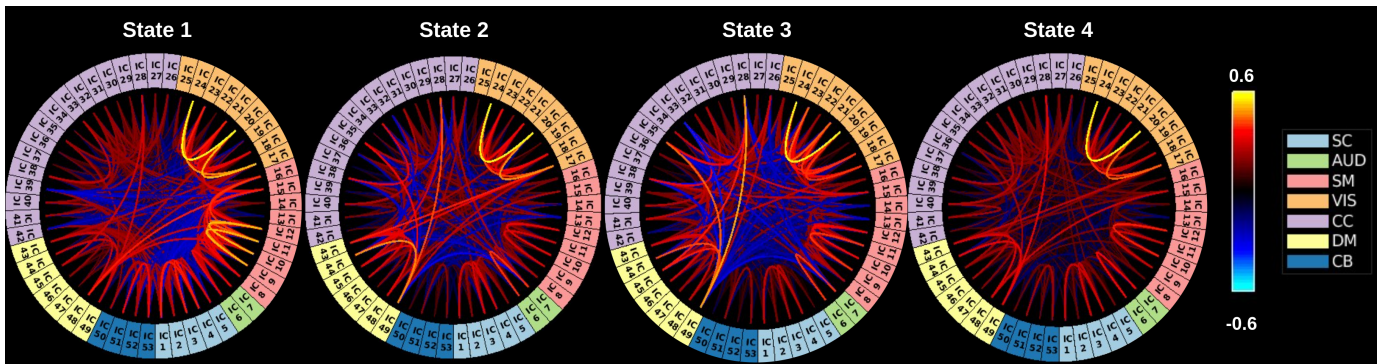


Fig. 1. **Discrete Functional Connectivity (FC) Patterns** (optimal number of brain states 4). These are the cluster centroids obtained through hard clustering analysis on the FC patterns from all subjects, both ASD and TD. The Connectograms depict the connectivity among the regions that comprise seven resting state networks indicated in different colors. The strengths of the inter-regional connectivity is depicted using a color map varying from -0.6 to 0.6.

graph theory among 33 HCs and 32 SCD subjects. [10] found 4 optimal dynamic brain states through hard clustering analysis on dFNC windows and identified hyperconnectivity within and between auditory domain, visual domain, and, somatomotor networks among SCD subjects. Fiorenzato et al. [11] analyzed the dFNC between 118 patients suffering with PD and 35 HCs. Two dynamic brain states have been found through the sliding window approach and hard clustering analysis. [11] hypothesized that the underlying cognitive deficits in PD subjects are characterized by strong connectivity in default mode and cognitive executive networks.

Contrasting with most extant studies, we compared dynamic brain states to sFNC. Specifically, the dynamic characteristics of the brain states were estimated while applying clustering analysis on the time series segments extracted from 7 brain networks consisting of 53 regions of interest on a large subset of 188 ASD and 195 TD subjects from the ABIDE-I consortium. This study aimed to (a) compare connectograms of ASD and TD subjects estimated with dFNC and sFNC (i.e., can dFNC delineate any other meaningful information in terms of brain network differences in addition to information that can be evident from sFNC?) (b) understand the dFNC based network group differences in each state and reveal the dFNC patterns that showed increased or decreased connectivity in ASD subjects, (c) explore the temporal properties such as fractional windows in each state, the mean dwell time of each state, and the number of transitions between each pair of dynamic states using statistical two-sample *T-test*.

II. METHODS

A. Extraction of Independent Component Networks

We used the ICA NeuroMark template [12] to extract 53 Independent Components (ICs) belonging to 7 resting state networks. The ICA NeuroMark Template is a functional parcellation atlas developed using independent component analysis (ICA) applied to rs-fMRI data. The atlas is based on data from a large sample of healthy individuals, and its regions of interest (ROIs) are defined by functional networks rather than anatomical boundaries. This approach allows for a

more precise mapping of functional connectivity networks in the brain and has the potential to reveal new insights into brain organization and function. The atlas is based on a standardized template space, which allows for easy comparison and integration with other neuroimaging datasets. The ICA NeuroMark Template has shown promise in diagnosing neurological disorders, such as Alzheimer's disease, Parkinson's disease, and multiple sclerosis. These networks were categorized into the following seven domains: Subcortical Domain (SC; ICs: 1–5), Auditory Domain (AUD; ICs: 6, 7), Visual Domain (VIS; ICs: 8–16), Somatomotor Domain (SM; ICs: 17–25), Cognitive Control domain (CC; ICs: 26–42), Default-Mode Domain (DM; ICs: 43–49), and Cerebellar Domain (CB; ICs: 50–53). ICA NeuroMark template can be downloaded here ¹ and its corresponding labels ². Time courses (TCs) are extracted from these ICNs followed by temporal pre-processing strategies that includes: detrending linear, quadratic, and cubic trends, despiking detected outliers, and low-pass filtering with cut-off frequency of 0.15 Hz.

B. Static Functional Connectivity estimation

sFNC is determined by computing the pair-wise Pearson correlation coefficient (PCC) between every pair of ICNs. The PCC, ρ_{xy} for two signals, x and y each of length T and mean \hat{x} and \hat{y} respectively, can be computed using the following equation.

$$\rho_{xy} = \frac{\sum_{t=1}^T (x_t - \hat{x})(y_t - \hat{y})}{\sqrt{\sum_{t=1}^T (x_t - \hat{x})^2} \sqrt{\sum_{t=1}^T (y_t - \hat{y})^2}} \quad (1)$$

Here, C represents the number of ICNs. sFNC obtained is a symmetric matrix of size $C \times C$, where each $(i, j)^{th}$ entry represents the PCC between i^{th} and j^{th} regions.

C. Dynamic Functional Connectivity estimation

A sliding window-based method was used to estimate dynamic Functional Network connectivity (dFNC) for each

¹NeuroMark Template

²NeuroMark Labels

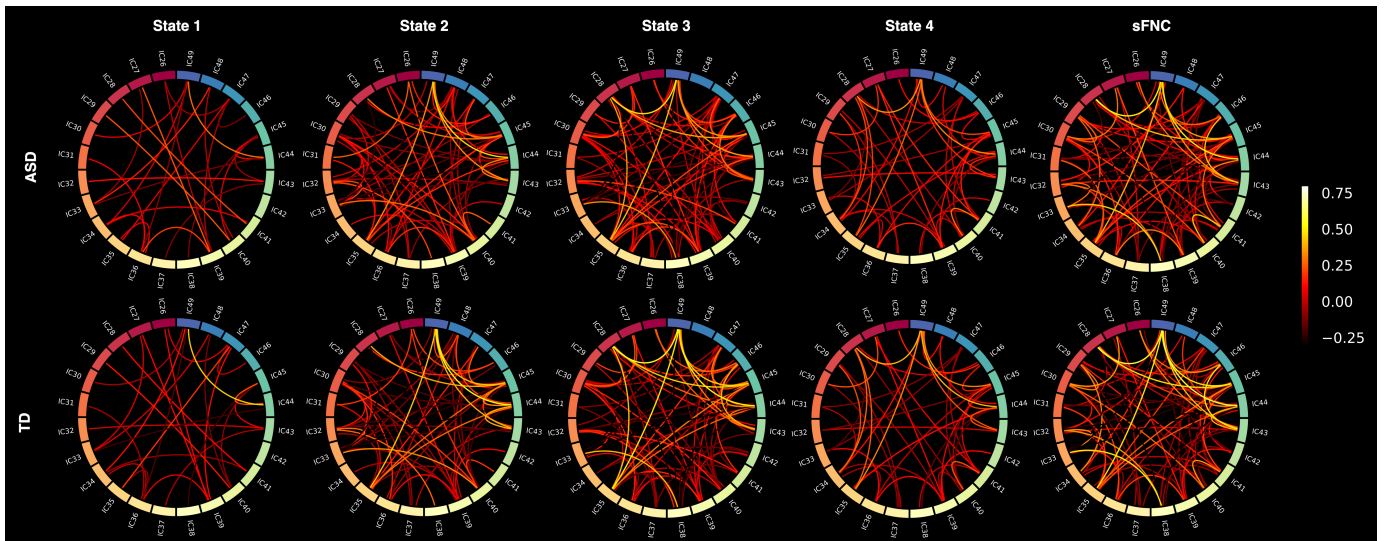


Fig. 2. **Connectograms of ASD vs TD and dFNC states vs sFNC.** Activations within and between CC and DM networks that are statistically significant in both groups ASD and TD. The first row represents the significantly stronger activations among ASD subjects and the second row represents significantly stronger activations among TD subjects in all four dynamic brain states. The last column represents the significantly stronger activations found in both groups found using sFNC analysis. The names of each IC and its corresponding brain networks are part of Neuromark template release.

TABLE I
DYNAMIC FUNCTIONAL CONNECTIVITY PARAMETERS

Parameters	Values
Number of components (C)	53
Timepoints per subject (T)	175
Window size (w)	20
Stride (s)	1
Windows extraction per subjects (N)	155
Windows extracted from all subjects (W)	59365

individual. We only chose the first T time points of each subject's component TCs for the dFNC estimation because the subject's data from different sites could have varying scan lengths. This was done to minimize the effects of different scan lengths. To localize the dataset at each time point, we created a tapered window by convolving a rectangle with a Gaussian ($\sigma = 3$). We chose a window size w TRs corresponding to t seconds. We slid the window in s TR increments, producing a total of N windows per subject. We estimated the regularised precision matrix using the graphical LASSO approach (with the $L1$ norm to encourage sparsity) and then deduced the covariance matrix from the precision matrix [13]. Let the total number of windows extracted from all the subjects be W . All the dFNC parameters can be seen in table I

D. Hard Clustering Analysis

The fundamental presumption behind the hard clustering state analysis is that functional brain networks will enter different states with unique dFNC patterns. All the windows extracted from all the subjects (W) are divided into distinct states (discrete FC patterns) utilizing the K-Means clustering technique and the $L1$ norm as the distance function. To reduce the redundancy between windows and computational demands,

we utilized the subset of windows (consisting of local maxima in functional connectivity variance) as subject exemplars. As K-means algorithm is sensitive to initialization, it was repeated for 100 times (with random initialization of centroid position) with a maximum of 250 iterations to obtain the group cluster centroids. To find the optimal number of states, we used the elbow criterion which is defined as the ratio of within clustering distance to between clusters distance. The optimal number of dynamic states was determined as $K = 4$. The optimal dynamic states can be seen in figure 1.

E. Group differences in static and dynamic-connectivity strength

Two-sample T -test analysis has been done to compare static and dynamic connectivity strength between ASD and TD groups. For dFNC, we repeated the below steps (A, B, C) for all four dynamic brain states. A) Consider those subjects in which at least a window belongs to that particular state. B) In all those subjects, compute the median of windows per state. C) There exist 1378 distinct connectivities for every pair of ICNs. For every distinct connectivity, performed the two-sample T -test between groups ASD and TD per state to find significantly different connectivities ($p < 0.05$, false discovery rate (FDR) correction). In case of sFNC, we can conduct the two-sample T -test directly on connectivity between pairs of ICNs to compare the groups.

F. Temporal properties

We also investigated the temporal properties of four dynamic brain states by computing the fractional windows (the number of total windows belonging to a given state), mean dwell time (the number of consecutive windows belonging to a given state) per state, and the number of transitions between each pair of states. Statistical two-sample T -test are used to

identify the differences between groups per state ($p < 0.05$, FDR correction).

TABLE II

DISTRIBUTION OF NUMBER OF SUBJECTS AND WINDOWS PER STATE FOR EACH GROUP: ASD AND TD. THE 'SUBJECTS' REPRESENTS THE NUMBER OF SUBJECTS OCCURRED IN EACH STATE, AND THE 'WINDOWS' REPRESENTS THE NUMBER OF WINDOWS ASSIGNED TO EACH STATE WITHIN ASD AND TD.

State	ASD		TD	
	Subjects	Windows	Subjects	Windows
State1	59	2241	79	3653
State2	145	5333	165	6575
State3	131	4849	158	6583
State4	185	16717	187	13414

III. DATASET & PREPROCESSING

The present work used the pre-processed dataset from the Autism Brain Imaging Data Exchange (ABIDE-1) initiative [14]. The dataset comprises 1,112 rs-fMRI scans acquired from 17 different sites. There exist 505 ASD and 530 Typical controls. For the analysis, we chose 383 subjects (188 ASD and 195 TD). The criteria to include subjects are as follows: 1) subjects with DSM-IV diagnosis, 2) subjects with mean frame-wise displacement (mFD) corresponding to two standard deviations above the sample mean, i.e., smaller than 0.4432, 3) subjects with at least 175, volumes in fMRI acquisition 4) subjects with repetition time (TR) = 2 sec while scanning 5) subjects with Full IQ score 6) subject mask with a spatial correlation greater than 0.8 with the group mask computed using the subjects qualified for the above five conditions. Group mask computation is as follows: Firstly, we determined the individual mask for each subject by setting the value of voxels larger than 70 percent of the entire brain mean value to 1. Next, we set the voxels present in more than 70% of the individual masks to 1 to compute a group mask. We used publicly available preprocessed four-dimensional rs-fMRI scans using Connectome Computation System (CCS) [15]. Dataset can be downloaded from here ³ by setting the pipeline as 'ccs' and strategy as 'nofilt_noglobal'.

IV. IMPLEMENTATION

ICNs extraction using ICA neuromark template, dFNC clustering analysis followed by hard clustering analysis and two sample T -test analysis has been done using Group ICA of fMRI Toolbox (GIFT) [16]. The toolbox scripts were implemented in matlab and can be downloaded from here ⁴. All the subject IDs of the ABIDE-I samples used in this paper, and parameters required to extract ICNs, estimate dFNC, and perform the clustering analysis will be made publicly available upon publication for reproducibility.

³Dataset

⁴GIFT toolbox

V. RESULTS

A. Characteristics of Different Brain States

Four optimal dynamic states have been found using K-Means clustering on all windows (W) extracted from all subjects in both ASD and TD. As shown in Table II, we can observe that 10% of the total windows were assigned to state 1 and characterized by strong positive intra-connectivity within VIS and SM networks and sparse connectivity within DM and CC networks. 20% of the windows were assigned to state 2 and characterized by strong positive intra-connectivity within VIS, DM networks and inter-connectivity between CC-DM networks. 19% of the windows were assigned to state 3 and characterized by strong positive intra-connectivity within VIS, SM, and inter-connectivity between CC-DM networks and negative inter-connectivity between AUD, SM, and CC networks. 51% of the windows were assigned to state 4 and characterized by positive intra-connectivity within SM, VIS, DM, and inter-connectivity between CC and DM. All the state characteristics mentioned above can be observed in figure 1. The group and state-specific distribution of windows and subjects can be seen in Table II. It is to be noted that not all the states occurred in all the subjects. From Table II, states 1 and 3 occurred less frequently among ASD subjects than in TD (state 1: ASD - 3.77%, TD - 6.15%; state 3: ASD - 8.16%, TD - 11.08%). State 4 occurred more frequently among ASD subjects (ASD - 28.15%, TD - 22.59%).

B. Dynamic Functional Connectivity Differences with two-sample T -test

For each state, Table III, shows the number of stronger connections in ASD and TD groups among pairs of within or between IC networks that are statistically significant ($p < 0.05$, FDR correction). Overall, for state 1, we observed 56 stronger within- and between-network connections in ASD compared to TD subjects. Similarly, for other states, 2, 3 and 4, the number of connections emerged to be higher in ASD compared to TD. Looking at the number of stronger connections among pairs of IC networks, we observed that within the CC network and between CC-DM networks, most of them were stronger in ASD subjects, whereas, within DM network, connections were stronger among TD individuals in all four states. Figure 2 highlights the qualitative visualization of regional differences in the CC-DM network. Interestingly, the patterns were quite similarly observed for static functional connectivity in ASD and TD groups, as evident from figure 2 focusing on the CC-DM network. However, the statistical comparisons on the temporal characterization of dynamic states (clusters) between ASD and TD brought additional regional differences between IC networks that may be evident in static functional connectivity or vice-versa. Overall, we observe 329 stronger intra- and inter-connectivity differences in ASD while using dynamic functional connectivity compared to 111 significant connections in ASD while using static functional connectivity.

TABLE III
DISTRIBUTION OF STRENGTH IN CONNECTIONS CHARACTERIZED FROM PAIRS OF IC NETWORKS FOR BOTH DYNAMIC AND STATIC FUNCTIONAL CONNECTIVITY. FOR EACH STATE, THE NUMBER INDICATES THE DOMINANT CONNECTIONS THAT ARE ESTIMATED FROM STATISTICAL DIFFERENCES WHILE COMPARING BOTH ASD AND TD GROUPS. FOR COMPARISON, WE ALSO SHOW STRENGTH IN CONNECTIONS EMERGED FROM STATIC FUNCTIONAL CONNECTIVITY.

State	Total		CC-CC		CC-DM		DM-DM		SM-CC		VIS-DM		VIS-CC		SC-CC	
	ASD	TD	ASD	TD	ASD	TD	ASD	TD	ASD	TD	ASD	TD	ASD	TD	ASD	TD
State1	56	40	8	2	8	5	0	4	10	2	1	0	8	7	4	7
State2	100	87	17	9	20	10	0	10	4	7	6	3	6	7	9	4
State3	103	94	21	13	21	14	0	13	1	5	17	2	6	18	2	6
State4	70	68	14	7	12	6	0	8	3	6	10	4	6	14	3	5
sFNC	111	114	19	16	24	18	0	12	4	6	9	5	7	9	2	11

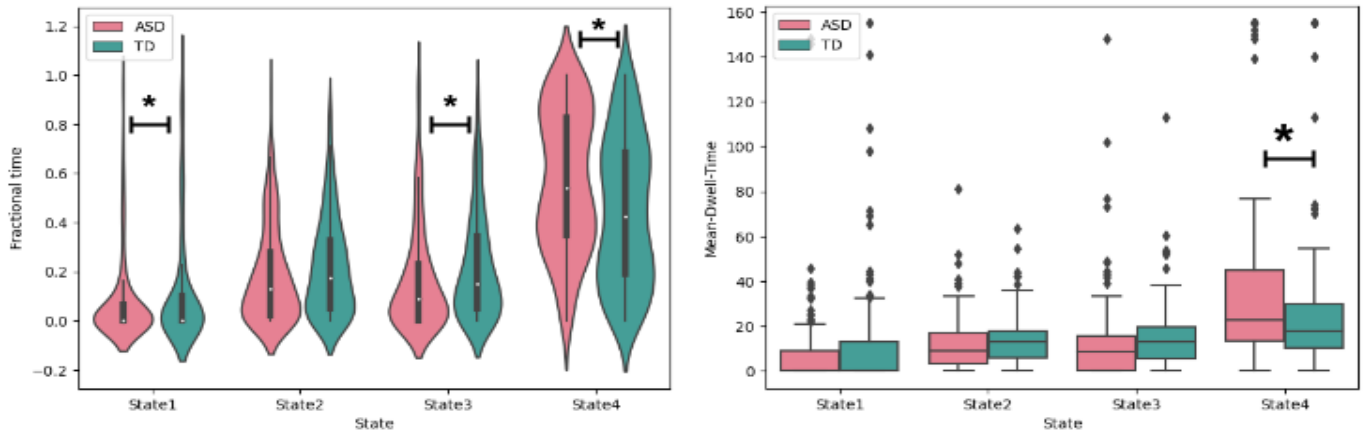


Fig. 3. **Fractional Time spent and Mean dwell time of ASD and TD groups per state.** The left plot represents the fractional time spent in each state and the right plot represents the mean dwell time of each state specific to the group. * indicate that the distributions are significantly different ($p < 0.05$, FDR correction)

C. Temporal Properties Differences

From figure 3, it can be observed that fractional time spent among ASD subjects is significantly greater than TD subjects in state 4 ($p = 0.0005$) and significantly lower in state 1 ($p = 0.04$) and state 3 ($p = 0.019$). Significant differences were found in mean dwell time of state 4. ASD subjects exhibited significantly longer mean dwell time in state 4 compared to TD subjects ($p = 0.00023$), while there was a trend for longer mean dwell time in state 3 among the TD subjects ($p = 0.071$). No significant differences between groups have been found based on the number of transitions between states (ASD: 6.27 ± 3.68 ; TD: 6.90 ± 3.17 ; $p = 0.071$, FDR correction). However, increasing trend can be observed among TD individuals.

VI. DISCUSSION

We studied dFNC patterns for ASD and TD on a large number of subjects sampled from the ABIDE-I consortium. We extracted dFNC patterns and applied hard clustering analysis on those patterns to find the optimal brain states or discrete FC patterns, which helps us to understand the network-level differences in the fundamental brain organization of ASD with respect to TD subjects. We performed a two-sample T -test and found many activations between ICNs within and between networks that are significantly different among the

groups ASD and TD per state ($p < 0.05$, FDR correction). We observed hyper-connectivity among ASD subjects within CC network and between CC-DM networks in all four states. Among TD subjects, hyper-connectivity has been found within DM network in all four states. The stability and occurrence of state 4 is significantly greater among ASD subjects when compared to TD individuals. The variability of the states revealed an increasing trend among TD individuals.

Regions that contribute to the hyper-connectivity in the CC network among ASD subjects in most of the dynamic states are found to be the Hippocampus, Middle cingulate cortex, Left inferior parietal lobule, Inferior frontal gyrus, and hypo-connectivity in the DM network are Precuneus, Posterior cingulate cortex, and Anterior cingulate cortex. The region hippocampus controls memory encoding, learning, and memory consolidation [17], the inferior frontal gyrus controls language comprehension and production [18], and the middle cingulate cortex is in charge of cognitive processing, particularly decision-making [19]. There are numerous neurological processes that the inferior parietal lobe (IPL) is assumed to be engaged in, such as spatial attention, multimodal sensory integration, and oculomotor control [20]. The precuneus is a part of the default mode network that performs a wide range of complicated tasks, such as information integration related to the perception of the environment, cue response, mental

imagery techniques, and retrieval of episodic memory [21]. The anterior and posterior cingulate cortex are responsible for social cognition [22], [23]. All of these functions are found to be effected in patients with ASD [24], [25].

Earlier research [26], [27] has investigated the role of altered FC of DM sub-networks among high-functioning ASD subjects based on rs-fMRI scans. These studies hypothesized that the FC between the precuneus and the medial prefrontal cortex/anterior cingulate cortex, and DM core areas were weaker in ASD patients. The findings are consistent with the concept that the fundamental deficiencies in ASD are a result of the under-connectivity of DM sub-networks [28]. Harlalka et al. [8] observed that patients with ASD demonstrated higher dFNC between the attentiveness network (AN) and default mode network (DM) than TD individuals.

The shortcoming of this study includes considering only male participants. This is to avoid gender-biased conclusions arising from our sample selection criteria. As future work, we extend this selection criterion to both males and females as gender influences in ASD subjects are proven to be different in terms of functional organization [29]. From a machine learning perspective, the connectivity strengths that are shown to be statistically significant (could act as a prior feature selection criteria) to classify ASD and TD. This may reveal the usefulness of dFNC over sFNC while considering the information from multiple brain states to averaged representation of sFNC. Within this space, another possible extension could be to correlate these hyper-connectivity findings in brain networks to clinical scores for a better understanding of sub-types such as Autistic, Asperger's, and Pervasive developmental disorder.

VII. CONCLUSION

In this paper, we studied the dFNC patterns from seven different brain networks between ASD and TD for Autism biomarkers. Our systematic comparisons across four optimal brain states revealed the hyper-connectivity within intra- and inter-level brain networks in ASD and TD. Examining the temporal properties revealed the stability and variability of states among ASD and TD. Though, the emerged dFNC networks are consistent with sFNC networks, our study ideates toward the detailed investigation of unique and overlapping brain network level differences arising from various inputs like timeseries with and without estimating functional connectivity can give more insights into disease biomarkers.

ACKNOWLEDGMENT

We thank iHub-Data, IIIT Hyderabad for the financial support.

REFERENCES

- [1] W. Lau, M. K. Leung, T. M. C. Lee, and A. C. K. Law, "Resting-state abnormalities in amnesic mild cognitive impairment: a meta-analysis," *Translational psychiatry*, vol. 6, no. 4, pp. e790–e790, 2016.
- [2] D. Vidaurre, S. M. Smith, and M. W. Woolrich, "Brain network dynamics are hierarchically organized in time," *Proceedings of the National Academy of Sciences*, vol. 114, no. 48, pp. 12 827–12 832, 2017.

- [3] J. Schumacher, L. R. Peraza, M. Firbank, A. J. Thomas, M. Kaiser, P. Gallagher, J. T. O'Brien, A. M. Blamire, and J.-P. Taylor, "Dynamic functional connectivity changes in dementia with lewy bodies and alzheimer's disease," *NeuroImage: Clinical*, vol. 22, p. 101812, 2019.
- [4] R. F. Betzel, M. Fukushima, Y. He, X.-N. Zuo, and O. Sporns, "Dynamic fluctuations coincide with periods of high and low modularity in resting-state functional brain networks," *NeuroImage*, vol. 127, pp. 287–297, 2016.
- [5] S. Shakil, C.-H. Lee, and S. D. Keilholz, "Evaluation of sliding window correlation performance for characterizing dynamic functional connectivity and brain states," *Neuroimage*, vol. 133, pp. 111–128, 2016.
- [6] Z. Fu, Y. Tu, X. Di, Y. Du, J. Sui, B. B. Biswal, Z. Zhang, N. de Lacy, and V. D. Calhoun, "Transient increased thalamic-sensory connectivity and decreased whole-brain dynamism in autism," *Neuroimage*, vol. 190, pp. 191–204, 2019.
- [7] L. Ma, T. Yuan, W. Li, L. Guo, D. Zhu, Z. Wang, Z. Liu, K. Xue, Y. Wang, J. Liu *et al.*, "Dynamic functional connectivity alterations and their associated gene expression pattern in autism spectrum disorders," *Frontiers in Neuroscience*, vol. 15, p. 1837, 2022.
- [8] V. Harlalka, R. S. Bapi, P. Vinod, and D. Roy, "Atypical flexibility in dynamic functional connectivity quantifies the severity in autism spectrum disorder," *Frontiers in Human Neuroscience*, vol. 13, p. 6, 2019.
- [9] Y. Li, Y. Zhu, B. A. Nguchu, Y. Wang, H. Wang, B. Qiu, and X. Wang, "Dynamic functional connectivity reveals abnormal variability and hyper-connected pattern in autism spectrum disorder," *Autism Research*, vol. 13, no. 2, pp. 230–243, 2020.
- [10] Q. Chen, J. Lu, X. Zhang, Y. Sun, W. Chen, X. Li, W. Zhang, Z. Qing, and B. Zhang, "Alterations in dynamic functional connectivity in individuals with subjective cognitive decline," *Frontiers in aging neuroscience*, vol. 13, p. 646017, 2021.
- [11] E. Fiorenzato, A. P. Strafella, J. Kim, R. Schifano, L. Weis, A. Antonini, and R. Biundo, "Dynamic functional connectivity changes associated with dementia in parkinson's disease," *Brain*, vol. 142, no. 9, pp. 2860–2872, 2019.
- [12] Y. Du, Z. Fu, J. Sui, S. Gao, Y. Xing, D. Lin, M. Salman, A. Abrol, M. A. Rahaman, J. Chen *et al.*, "Neuromark: An automated and adaptive ica based pipeline to identify reproducible fmri markers of brain disorders," *NeuroImage: Clinical*, vol. 28, p. 102375, 2020.
- [13] J. Friedman, T. Hastie, and R. Tibshirani, "Sparse inverse covariance estimation with the graphical lasso," *Biostatistics*, vol. 9, no. 3, pp. 432–441, 2008.
- [14] A. Di Martino, C.-G. Yan, Q. Li, E. Denio, F. X. Castellanos, K. Alaerts *et al.*, "The autism brain imaging data exchange: towards a large-scale evaluation of the intrinsic brain architecture in autism," *Molecular psychiatry*, vol. 19, no. 6, pp. 659–667, 2014.
- [15] T. Xu, Z. Yang, L. Jiang, X.-X. Xing, and X.-N. Zuo, "A connectome computation system for discovery science of brain," *Science Bulletin*, vol. 60, no. 1, pp. 86–95, 2015.
- [16] S. Rachakonda, E. Egolf, N. Correa, and V. Calhoun, "Group ica of fmri toolbox (gift) manual," *Dostupnez [cit 2011-11-5]*, 2007.
- [17] K. S. Anand and V. Dhikav, "Hippocampus in health and disease: An overview," *Annals of Indian Academy of Neurology*, vol. 15, no. 4, p. 239, 2012.
- [18] B. Ishkhanyan, V. Michel Lange, K. Boye, J. Mogensen, A. Karabanov, G. Hartwigsen, and H. R. Siebner, "Anterior and posterior left inferior frontal gyrus contribute to the implementation of grammatical determiners during language production," *Frontiers in Psychology*, vol. 11, p. 685, 2020.
- [19] F. R. Jumah and R. H. Dossani, "Neuroanatomy, cingulate cortex," 2019.
- [20] D. M. Clower, R. A. West, J. C. Lynch, and P. L. Strick, "The inferior parietal lobule is the target of output from the superior colliculus, hippocampus, and cerebellum," *Journal of Neuroscience*, vol. 21, no. 16, pp. 6283–6291, 2001.
- [21] A. E. Cavanna and M. R. Trimble, "The precuneus: a review of its functional anatomy and behavioural correlates," *Brain*, vol. 129, no. 3, pp. 564–583, 2006.
- [22] F. L. Stevens, R. A. Hurley, and K. H. Taber, "Anterior cingulate cortex: unique role in cognition and emotion," *The Journal of neuropsychiatry and clinical neurosciences*, vol. 23, no. 2, pp. 121–125, 2011.
- [23] R. Leech and D. J. Sharp, "The role of the posterior cingulate cortex in cognition and disease," *Brain*, vol. 137, no. 1, pp. 12–32, 2014.

- [24] M. Solomon, J. B. McCauley, A.-M. Iosif, C. S. Carter, and J. D. Ragland, "Cognitive control and episodic memory in adolescents with autism spectrum disorders," *Neuropsychologia*, vol. 89, pp. 31–41, 2016.
- [25] I. P. Levin, G. J. Gaeth, M. Foley-Nicpon, V. Yegorova, C. Cederberg, and H. Yan, "Extending decision making competence to special populations: a pilot study of persons on the autism spectrum," *Frontiers in Psychology*, vol. 6, p. 539, 2015.
- [26] M. Assaf, K. Jagannathan, V. D. Calhoun, L. Miller, M. C. Stevens, R. Sahl, J. G. O'Boyle, R. T. Schultz, and G. D. Pearlson, "Abnormal functional connectivity of default mode sub-networks in autism spectrum disorder patients," *Neuroimage*, vol. 53, no. 1, pp. 247–256, 2010.
- [27] B. Yang, M. Wang, W. Zhou, X. Wang, S. Chen, M. N. Potenza, L.-x. Yuan, and G.-H. Dong, "Disrupted network integration and segregation involving the default mode network in autism spectrum disorder," *Journal of Affective Disorders*, vol. 323, pp. 309–319, 2023.
- [28] K. Supekar, S. Ryali, R. Yuan, D. Kumar, C. de Los Angeles, and V. Menon, "Robust, generalizable, and interpretable artificial intelligence-derived brain fingerprints of autism and social communication symptom severity," *Biological Psychiatry*, vol. 92, no. 8, pp. 643–653, 2022.
- [29] K. Supekar, C. de Los Angeles, S. Ryali, K. Cao, T. Ma, and V. Menon, "Deep learning identifies robust gender differences in functional brain organization and their dissociable links to clinical symptoms in autism," *The British Journal of Psychiatry*, vol. 220, no. 4, pp. 202–209, 2022.